Indian Journal of Radio & Space Physics
Vol 49, December 2020, pp 197-209

Assessment of geomagnetic storm effects over Ethiopian ionosphere by using GPS measurements

Z Legesse Mekonnen [a] & T Lake Endeshaw[b,c*]

[a]Department of Physics, Debark University, Debark, Ethiopia

[b]Department of Physics, Worabe University, Worabe, P.O.Box 46, Ethiopia

[c]Department of Space Science and Application Research and Development (SSARD), Ethiopian Space Science and Technology Institute (ESSTI), Addis Ababa University, Addis Ababa, Ethiopia

Received: 19 July 2020 Accepted: 13 October 2020

In this paper we have investigated the effects of geomagnetic storm on the variation of interplanetary magnetic field (IMF Bz), disturbance storm time (Dst), solar wind speed and total electron content (TEC) over Ethiopian ionosphere. A total of 17 geomagnetic storms have analysed by using ground based Global Positioning System (GPS) stations at Bahir Dar (11^o N, 38^o E), Debark(4.32^o N, 109.48^o E), Armi (3.03^o N, 109.29^o E), Nazret (8.57^o N, 39.29^o E), Robe(7.60^o N, 40^{o}E), Assosa (1.14^o N, 106.16^o E), and Ambo(8.59^o N, 37.51^o E) from the years 2010 to 2013. The results have revealed that there is a mixed effect of geomagnetic storm on the variation of interplanetary magnetic field (IMF Bz), disturbance storm time (Dst), solar wind speed and total electron content (TEC), however, most of the effects were positive and might be attributed to the prompt penetration electric fields (PPEFs) and disturbed dynamo fields.

Keywords: Disturbance storm time (Dst), Interplanetary magnetic field (IMF Bz), Solar wind speed (sws), Total electron content (TEC)

1 Introduction

A geomagnetic storm (GMS) is a temporary disturbance of the Earth's magnetosphere caused by a solar wind shock wave or cloud of magnetic field that interacts with the Earth's magnetic field. The increase in solar wind pressure initially compresses the magnetosphere[1,2]. The solar wind's magnetic field interacts with the Earth's magnetic field and transfers an increased energy into the magnetosphere. A geomagnetic storm has three phases an initial phase, a main phase and a recovery phase. The initial phase is characterized by Dst increasing by 20 to 50 nT in tens of minutes. The initial phase is also referred to as a storm sudden commencement (SSS)[3,4]. The main phase of a geomagnetic storm is defined by Dst decreasing to less than -50 nT. The recovery phase is the period Dst changes from its minimum value to its quiet value[5].

The Dst index estimates the globally averaged change of the horizontal component of the Earth's magnetic field at the magnetic equator based on measurements from a few magnetometer stations[6,7,8]. Dst is an indicator of magnetic disturbance intensity and development. Loewe and Prolss[9] classify GMS based on the minimum Dst valve, as weak (-30 to -50 nT), moderate (-50 to -100 nT), intense (-100 to -200 nT), severe (-200 to -350 nT) and great (less than -350 nT). In addition to the Dst index as a measure of geomagnetic disturbance, the Aurora Electro Jet (AEJ), the ap, the K and Kp indexes are often used[10,11,12,13].

The Total Electron Content (TEC) is the amount of free electrons along the path of the electromagnetic wave in a particular line of sight[14]. The TEC in the ionosphere modified by changing solar extreme ultraviolet radiation, geomagnetic storms and atmospheric waves that propagate up to from the atmosphere. Therefore, the TEC will depend on geomagnetic conditions and geomagnetic storm effects. The disturbances may be limited to the high-latitude polar region, unless the interplanetary magnetic field (IMF) carried by the solar wind has several hours of southward component (Bz < 0) with large magnitudes. The occurrence of such a period stresses the magnetosphere continuously, causing the magnetic field disturbance to reach the equatorial region. The degree of the equatorial magnetic field deviation is usually given by the Dst index. This is the hourly average of the deviation of horizontal component of the magnetic field measured by several ground stations in mid to low-latitude[15].

Several studies showed that the effects of geomagnetic storms in terrestrial infrastructures, the Earth's atmosphere and Earth's ionosphere. Zhao et al.[16] have studied the equatorial ionization anomaly (EIA) response in China, South-East Asia and Australian regions by using multi-instrument data during October to November 2003 super storm and found that large magnetic disturbances when EIA undergoes a short lived drastic change. The results of Maruyama et al.[13] showed that at the early stage of the storm (t < 12 hr.) and daytime penetration effect is dominant which have longer lifetime when the IMF Bz is larger and negative. During the night-time both prompt penetration and disturbance dynamo effects are comparable; but at the later stage daytime penetration field is less likely to follow the solar wind and IMF variations. And also Manju et al.[17] have studied during the 29 October super storm movement of the anomaly crest towards higher latitudes corresponding to the time enhanced vertical plasma drifts and the potentially significant effect of the meridional winds in the late afternoon hours at low latitude regions in the Indian longitude sector. Rama Rao et al.[18] have studied in the Indian sector two overlapping geomagnetic storms occurred during 8 to 12 November and found that the negative effects on the GPS range delay measurements as inferred from TEC measurements made from dual frequency GPS receivers. Astafyeva[19] has studied that the effects of strong IMF Bz southward events on the equatorial and mid-latitude ionosphere and conclude that the responsible for super-storm formation and occurrence of ionosphere storm-time effects is no an unambiguous answer for the question of preferred longitude sector during storms of 18 June 2003, 11 February 2004 and 24 August 2005. Woodroffe et al.[10] have studied that latitudinal distribution of peak geo-electromagnetic disturbances amplitudes during large (Dst < -100 nT) geomagnetic storms and found that extreme storms pose the greatest risk for lower latitudes and it is not the case in high latitudes.

The main objective of this study is to investigate the largest statistical assessment of geomagnetic storm response over Ethiopian ionosphere by using GPS measurement methods during all geomagnetic storms from 2010 to 2013. By using this storm data we have examined the effect of geomagnetic storm on the variation of interplanetary magnetic field (IMF Bz), disturbance storm time (Dst), solar wind speed and total electron content (TEC). Different from the previous study, we observed by considering a geomagnetic storm day with a minimum of Dst index (-50 nT) occurred in the four years of months at seven GPS stations in different geographic locations. Hence, this is perhaps the first work to extensively assess the geomagnetic storm effects on the variation of interplanetary magnetic field (IMF Bz), disturbance storm time (Dst), solar wind speed and total electron content (TEC) over Ethiopian ionosphere.

2 Methods

We have analysed the events represented by maximum Dst decrease and selected by using the selection procedure[9]. A list of magnetic storms are based on the Dst indexes provided by the World Data Centre for Geomagnetism, Kyoto, Japan through its world wide web and also from the Omni web data source maintained by National Geophysical Data Centre (NGDC) is being compiled for this study. The Omni Web Data results were used to identify the geomagnetic storm periods, the storm criterion of Dst ≤ -50 nT was selected based on Vijaya et al.[20] and the Dst data downloaded from the World Data Centre in Kyoto[1]; the Halo CMEs data in Solar and Heliospheric Observatory (SOHO) were obtained[2]. The geomagnetic storms have been analysed by using ground-based Global Positioning System (GPS) receivers namely Bahir Dar (11^o N, 38^o E), Debark (4.32^o N, 109.48^o E), Armi (3.03^o N, 109.29^o E), Nazret (8.57^o N, 39.29^o E), Robe (7.60^o N, 40^{o}E), Assosa (1.14^o N, 106.16^o E) and Ambo (8.59^o N, 37.51^o E) and each storm period were then extracted at 1 hour daily intervals using the standard archiving output explorer software (MATLAB). Over the stations, the collected GPS receiver's observations were to derive TEC with the software obtained during the period 2010-2013 observations.

3 Results and Discussions

3.1 Storm of 2010

3.1.1 Storm of February 14 2010

From observations of LASCO in February 12, 2010 at 1342 UT a halo Coronal Mass Ejections (CMEs) event with 360^o apparent width travels at a speed of 509 km/s and causes a geomagnetic storm on February 14 (DOY = 46), 2010. Figures 1, 2 and 3 show yearly variations of 2010 geomagnetic activity indexes, speed of solar wind, IMF Bz and the vTEC over Bahir Dar, Nazret and Robe respectively. The storm stared with SSC at 1900 UT on February 14, 2010 with a southward Bz attains a minimum value of

-8.6 nT. The effect of this turning has contributed to the decrease of the horizontal component of the Earth's magnetic field to the point where the minimum Dst value reached -59 nT (moderate geomagnetic storm) at 2300 UT. After 2330 UT, Bz shows a rapid increase in the northward direction and attains 4 nT at 1600 UT on February 15, 2010.

For the analysis of February 14, 2010 storm during the initial phase and part of the main phase of this storm the day time vTEC shows a positive response (about 35 TECU enhancement around 1000-1500 UT) followed by negative response in the post-sunset period a short enhancement of vTEC values at Bahir Dar, Nazret and Robe. In night-time (at 2321 UT) shows negative response of vTEC as shown in Figures 1, 2 and 3. In afternoon period and mid-night period, show a significant positive response (about 30 TECU). Post-midnight and

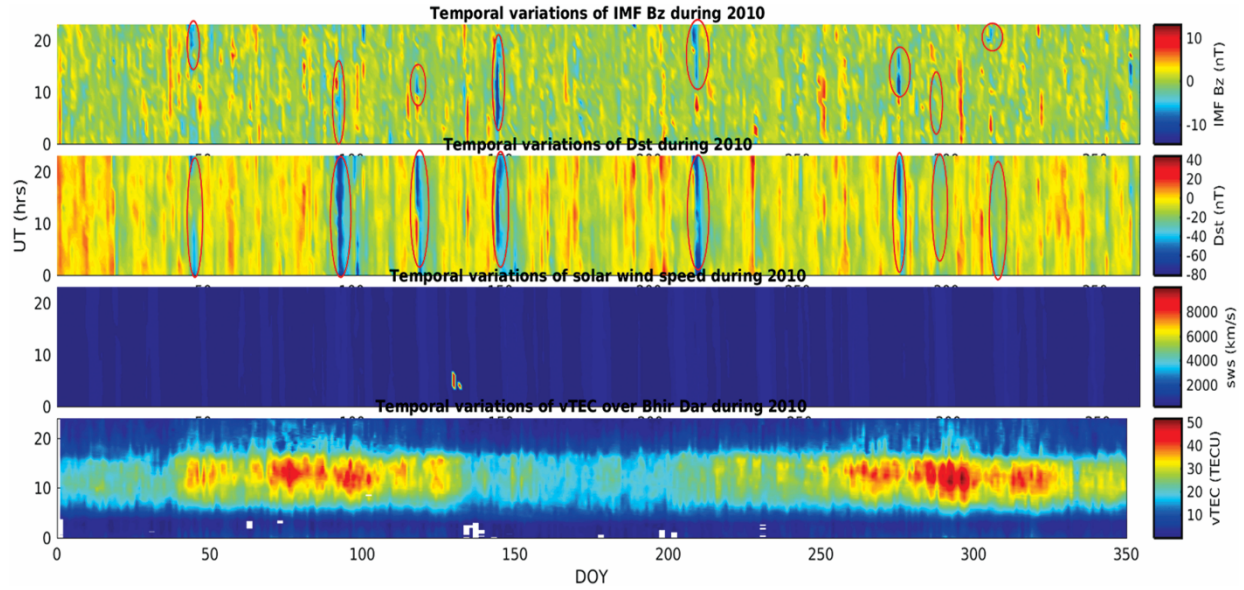

Fig. 1 — The variations of the Bz, Dst, solar wind speed and vTEC over Bahir Dar in 2010. The circle in the figure shows the increment of IMF Bz and Dst index.

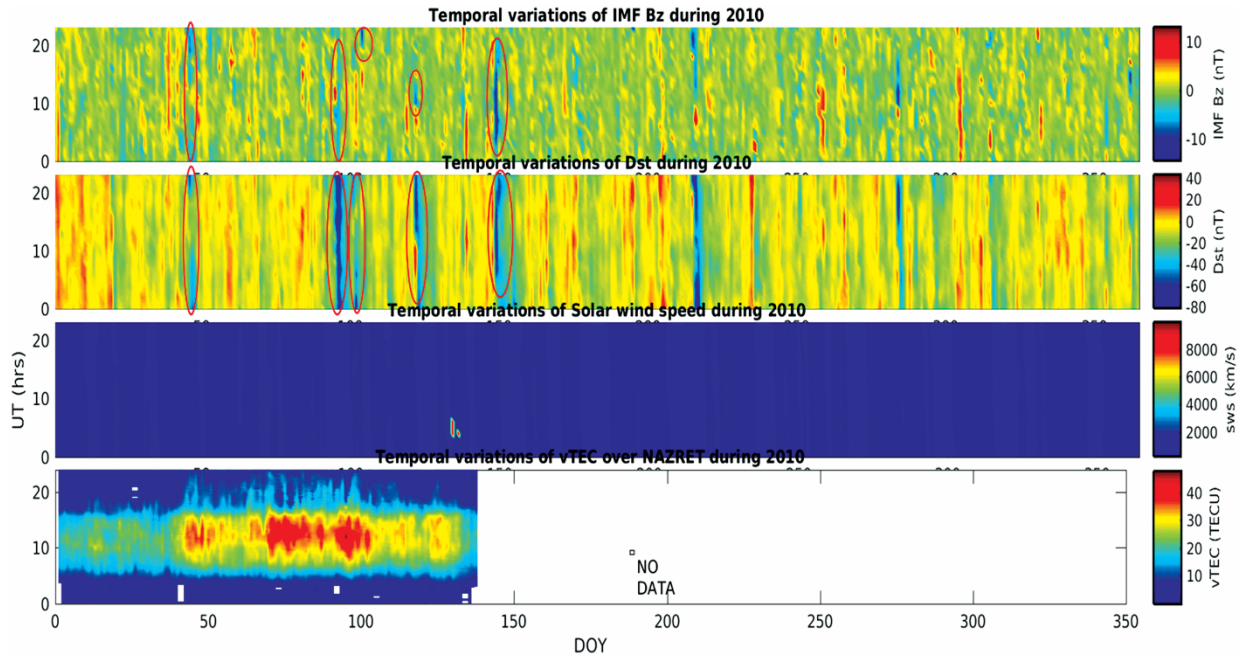

Fig. 2 — The variations of Bz, Dst, solar wind speed and the vTEC over Nazret in 2010. The circle in the figure shows the increment of IMF Bz and Dst index.

morning periods show negative response on February 14, 15 and 16.

3.1.2 Storm April 6, 2010

The high solar wind speed was appeared on April 5 (DOY= 95) at 1400 UT and solar wind starts increment on April 4 at 2300 UT, The solar wind velocity increased by 287 km/s and Bz changes from near zero to almost -6.7 nT at 0500 UT. The large values of Bz in the solar wind led to enhanced reconnection on the day side and enhanced magnetospheric convection. After some rapid fluctuations, the IMF Bz initially dropped to -81 nT (moderate geomagnetic storm) at 1400 UT on May 6, 2010.

3.1.3 Storm of May 7-9, 2010

The main phase of the storm stared after 13 hours from the SSC time in May 7, (DOY=149) 2010. Bz turns southward at 0102 UT from a northward configuration and attains a maximum value of -13.8 at 1100 UT. Such a sudden Bz drop caused an intense geomagnetic storm with Dst value of -80 nT at 1200 UT on May 7, 2010 and following the maximum southward orientation of Bz on May 7, 2010. The main phase of the storm was on May 7 and 8, the recovery phase was on May 9 at 2000 UT when the IMF turns to northward and the Dst become less negative (-35 nT) at 2300 UT. For the analysis of the storm on May 7-9, 2010 during the initial phase and part of the main phase of this storm, the daytime vTEC shows a negative response (about 18 TECU enhancements) during and after the storm enhancement of vTEC values at Bahir Dar, Robe, but have no vTEC data at Nazret. In morning period and post-midnight period, show a significant positive response (about 30 TECU); mid-night and afternoon periods show negative response deviation as shown in Figs 1, 2 and 3.

3.1.4 Storm of August 4, 2010

The large values of Bz in the solar wind led to enhanced reconnection on the day side and to enhanced magnetospheric convection. The solar wind velocity increased by 123km/s and Bz changes from near zero to almost -10 nT. After some rapid fluctuations the IMF Bz remained southward for a long period and exhibited a number of oscillations. These oscillations reflected in the variations of geomagnetic field component. The initial phase of the storm started with sudden commencement on August 3, 2010 at 2100 UT. After the initial phase, Dst started becoming more negative during the main phase and reached -74 nT at 0100 UT on August 4, (DOY=216) 2010. IMF Bz remained southward for almost for three days and then turned northward. For the analysis of August 4, 2010 storm during the initial phase and part of the main phase of this storm, the day time vTEC shows a positive response (about 30 TECU enhancement) during and after the storm enhancement of vTEC values at Bahir Dar, Robe and have no vTEC data at Nazret as shown in Figs 1, 2 and 3.

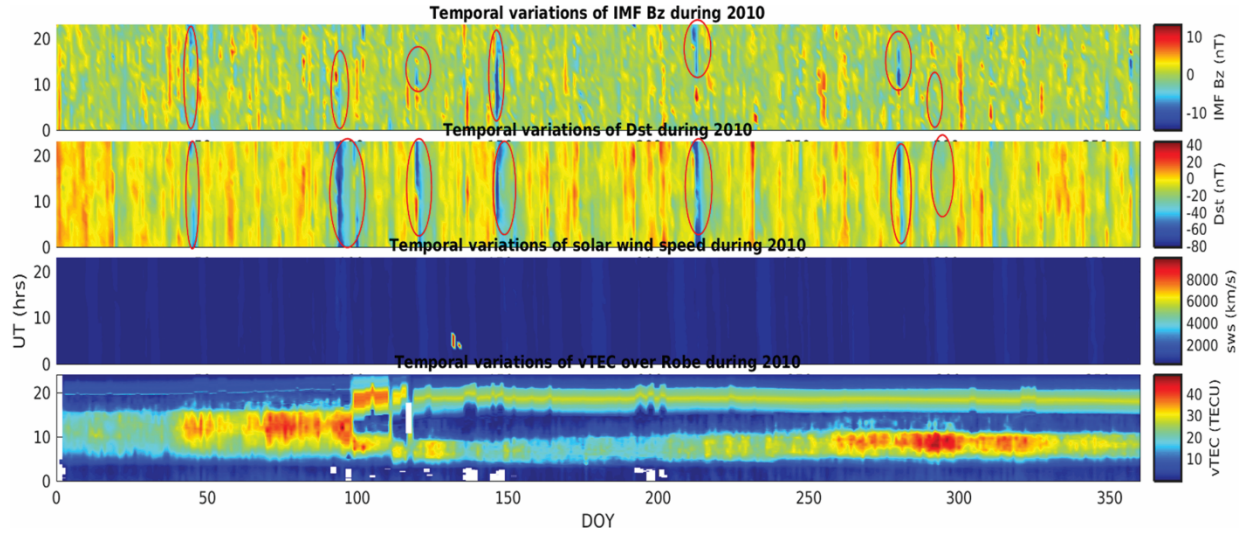

Fig. 3 — The variations of Bz, Dst, solar wind speed and vTEC over Robe in 2010. The circle in the figure shows the increment of IMF Bz and Dst index.

3.2 Storm of 2011

3.2.1 Storm of March 8, 2011

An interplanetary shock headed towards Earth is detected by wind around 1800 UT on March 7, (DOY=69) 2011. This shock caused by a solar coronal mass ejection observed by SOHO at 2000 UT on March 7, 2011. The solar wind was strong (<2125 km/s) that it compressed the magnetosphere and triggered a great geomagnetic storm. The initial phase of the storm started with a sudden commencement on March 8, 2011 at 0100 UT. After the initial phase, Dst stared becoming more negative during the main phase and reached -83 nT at 0500 UT on March 8, 2011. IMF Bz remained southward for almost -10.7 nT at 0200 UT for almost 10 hours with southward and then turned northward on March 9 at 0100 UT. The daytime vTEC show a positive response (about 40 TECU enhancement around 1000-1500) followed by negative response in post-sunset period a short enhancement of vTEC values at Bahir Dar, Robe and Nazret was observed.

3.2.2 Strom of August 5-6, 2011

The solar wind was strong (<620 km/s) that it compressed the magnetosphere. The initial phase of the storm started with a sudden commencement on August 5 (DOY=217) at 2100 UT. After the initial phase, Dst started becoming more negative during the main phase and reached -115 nT (intense geomagnetic storm) at 0300 UT on August 6, 2011. IMF Bz remained southward for almost -18.7 nT at 2100 UT for almost 10 hours with southward and the turned northward on August 6, 2011 at 0800 UT. For the analysis of August 5-6, 2011 storm during the initial phase and part of the main phase of this storm the daytime vTEC shows a negative response (about 20 TECU enhancements) vTEC values at Bahir Dar, Nazret and Arba Minch as shown in Figures 4, 5 and 6.

3.2.3 Storm of September 26, 2011

The solar coronal mass ejection observed by SOHO at 1936 UT on September 24, 2011 caused a great geomagnetic storm. The solar wind was so strong (972 km/s) that it compressed the magnetosphere. The initial phase of the storm started with a sudden commencement on September 26, (DOY=269) 2011 at 1800 UT and Dst started becoming more negative during main phase and reached -118 nT (intense geomagnetic storm) at 2300 UT on September 26, 2011. The IMF Bz value is -16.4 nT at 1800 UT and vTEC shows a positive response (about 60 TECU enhancement around between 1000- 1500 UT) followed by negative in the post-sunset period a short enhancement of vTEC values at Nazret and Arba Minch was observed, but we didn't have vTEC data for Bahir Dar.

3.2.4 Storm of October 25, 2011

The solar coronal mass ejection observed by SOHO at 1024 UT on October 22, 2011. The solar wind was strong (1005km/s) that it is compressed the magnetosphere. The Dst in the main phase become more negative -144 nT (intense geomagnetic storm) at 0100 UT on October 25, 2011. The IMF Bz value is -10.7 nT at 0100 for almost 2 hours and vTEC shows a positive response (about 70 TECU enhancement

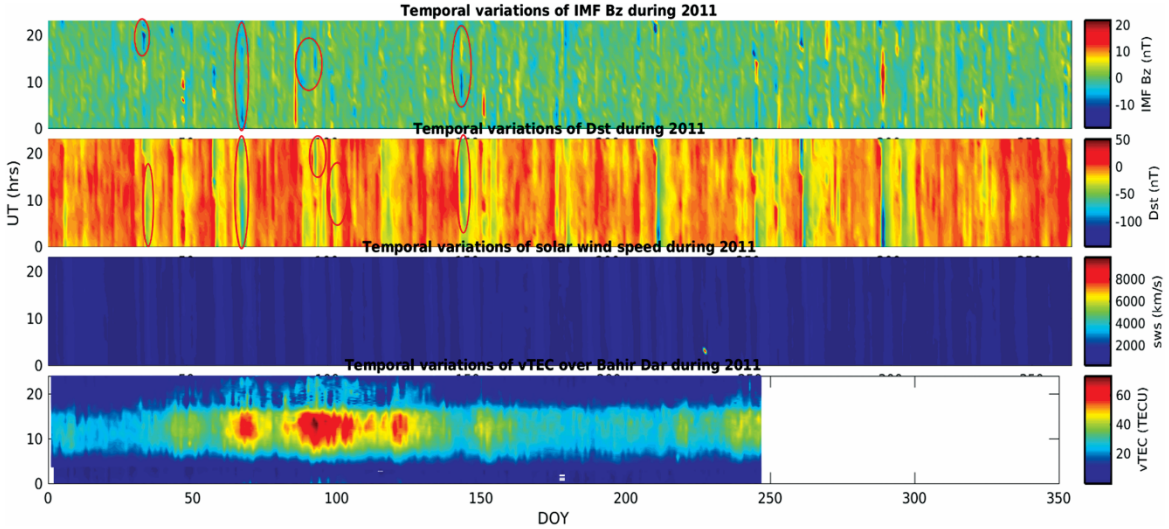

Fig. 4 — The variations of Bz, Dst, solar wind speed and the vTEC over Bahir Dar in 2011. The circle in the figure shows the increment of IMF Bz and Dst index.

around between 1000 - 1500 UT); followed by negative in the post-sunset period a short enhancement of vTEC values at Nazret and Arba Minch observed, but we didn't have vTEC data for Bahir Dar as shown in Figs 4, 5 and 6.

3.3 Storm 2012

3.3.1 Storm of March 7-9, 2012

Two full width halo CME events observed on March 5 at 0400 UT with speed of 1531 km/s and on March 7 at 0024 UT with speed 2684 km/s that strike the Earth on March 8, 2012. The storm of March 7 (DOY=67) started with SSC at 0420 UT. The Solar wind speed shows a sharp increment with a value of 441 km/s at 0820 UT followed by further sharp increment after few hours of steady values. Bz turns southward significantly after SSC with a value of 12.8 nT at 0500 UT. This leads to a geomagnetic storm of -98 nT at 0900 UT. After an hour Bz turns southward again and reaches a value of -19 nT at 1620 UT and then turns northward at 1820 UT. After a short recovery of March 7 storm, the second halo event

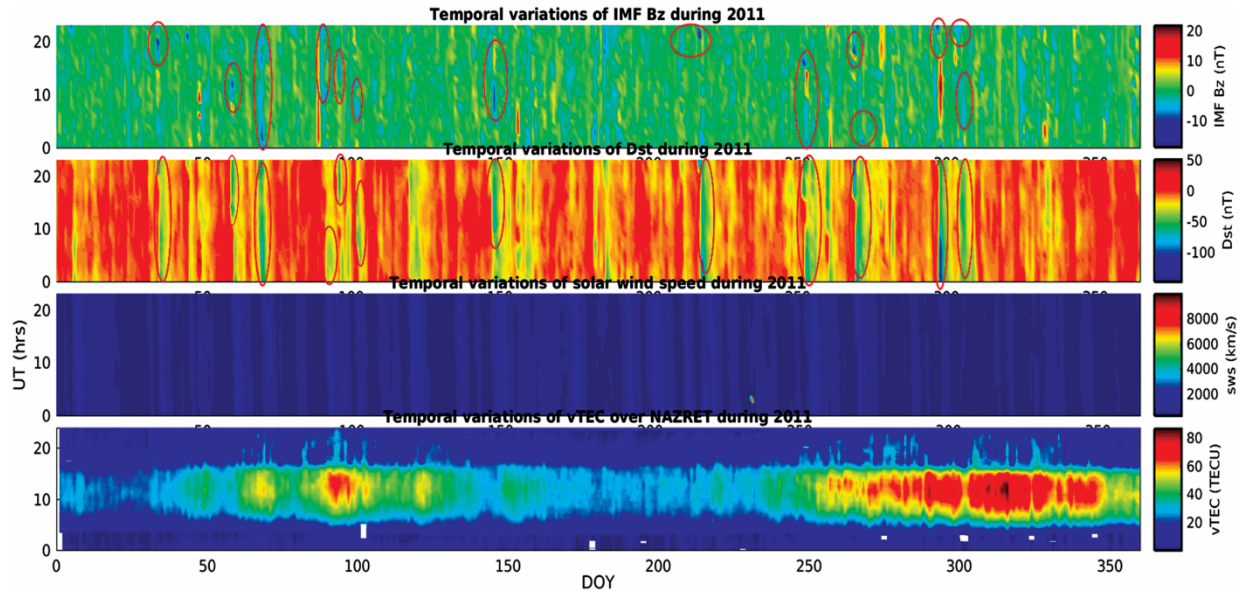

Fig. 5 — The variations of Bz, Dst, solar wind speed and the vTEC over Nazret in 2011. The circle in the figure shows the increment of IMF Bz and Dst index.

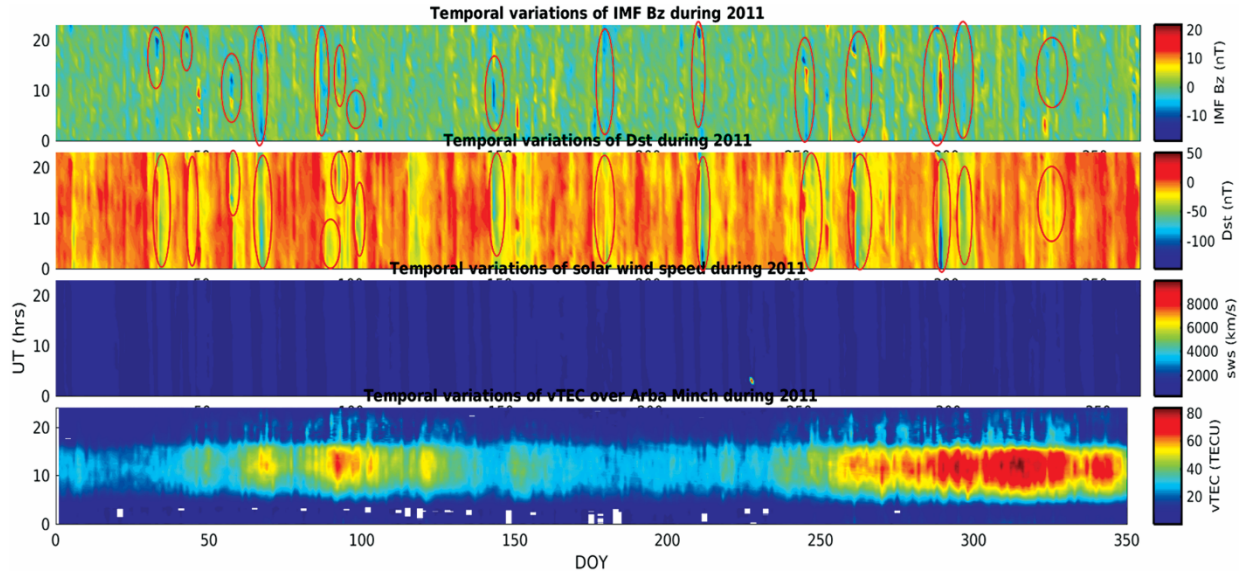

Fig. 6 — The variations of Bz, Dst, solar wind speed and the vTEC over Arba Minch in 2011. The circle in the figure shows the increment of IMF Bz and Dst index.

observed on Mar 7, 2012 creates another storm on March 8, 2012 that started with SSC at 1103 UT with a fast solar wind speed about 794 km/s. The IMF Bz turns northward about 19 nT at 1120 UT and later 20 UT at 1930 UT. The main phase of the storm stared after several hours from the SSC time on March 9, 2012. Bz starts turns southward and attains a maximum value of -18.5 nT at 0930 UT. This leads to a minimum value of Dst index -145 nT at 1320 UT. In the day time vTEC shows a positive response (about 55 TECU) and in the post-sunset period a short enhancement of vTEC values at Bahir Dar, Arba Minch (ARMI), Ambo, Assosa and Debark observed as shown in Figs 7, 8, 9, 10 and 11 respectively.

3.3.2 Storm of April 23, 2012

The initial phase of the storm started with a sudden commencement on April 23, (DOY=114) 2012 at 1800 UT. During the main phase, the Dst reached -106 nT (intense geomagnetic storm) at 2300 UT on April 23, 2012. Bz starts turning southward at 1400 UT and attains a maximum value of -14.7 nT at 1900 UT. The IMF Bz value is -10.7 nT at 0100 UT and in the day time vTEC shows a positive response (about 55 TECU) followed by negative response in the post-

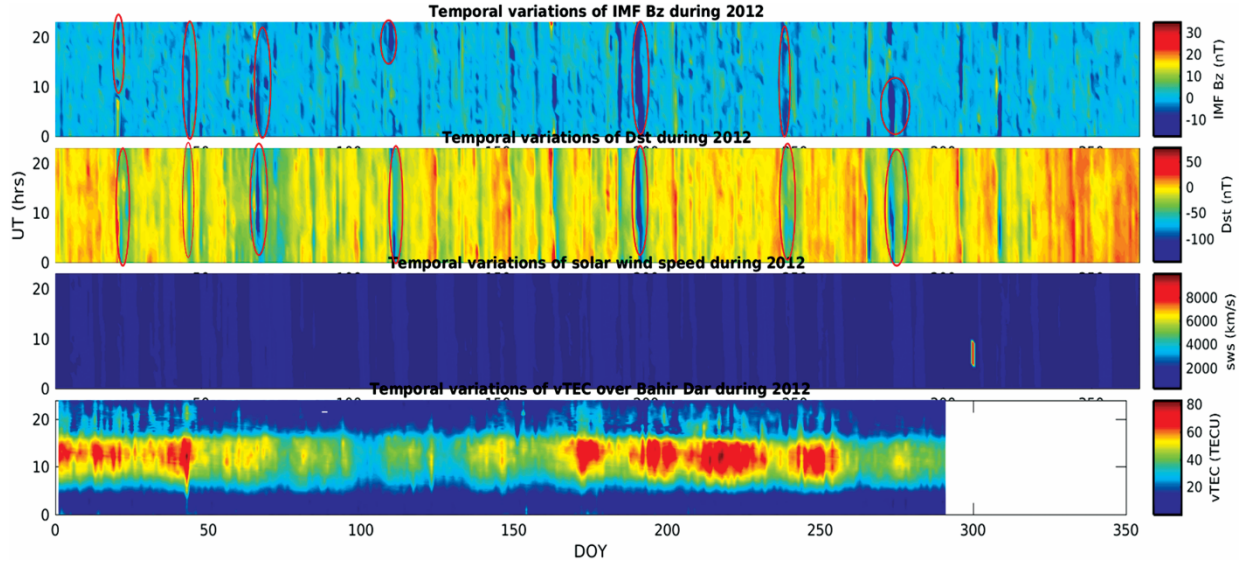

Fig. 7 — The variations of Bz, Dst, solar wind speed and the vTEC over Bahir Dar in 2012. The circle in the figure shows the increment of IMF Bz and Dst index.

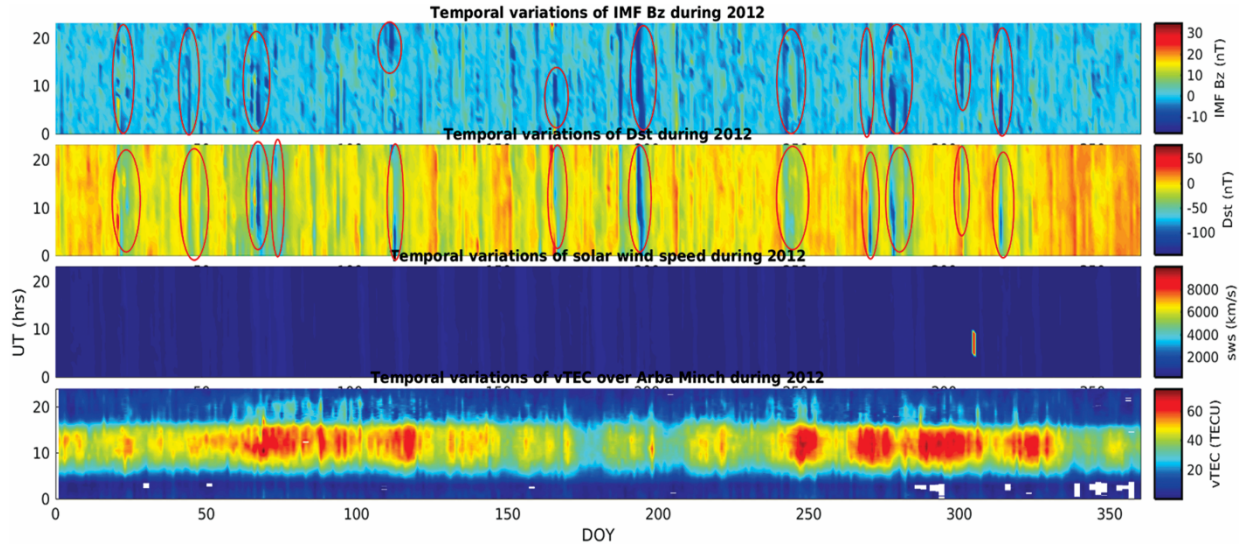

Fig. 8 — The variations of Bz, Dst, solar wind speed and the vTEC over Arba Minch in 2012. The circle in the figure shows the increment of IMF Bz and Dst index.

sunset period at Bahir Dar, Arba Minch, Ambo, Asosa and Debark was observed.

3.3.3 Storm of July 15-16, 2012

The initial phase of the storm started with a sudden commencement on July 15, (DOY=197) at 0900 UT and the Dst in the main phase is -139 nT at 1600 on July 15, 2012. The Bz starts turning southward at 0600 UT and attains a maximum value of -17.7 nT at 1000 UT. IMF Bz remained southward for almost 15.3 nT for about 8 hours with southward and then turned to northward on July 17 at 1000 UT. Storm of July 15-16, 2012 during the initial phase and main phase at day time, vTEC shows a positive response (about 55 TECU enhancement around between 1000-1500 UT) followed by negative response in the post-sunset period a short enhancement of vTEC values at Bahir Dar, Arba Minch, Ambo, Asosa and Debark was observed. In the night-time (2321 UT) shows a negative response of vTEC as shown in Figs 7, 8, 9, 10 and 11.

3.3.4 Storm of October 8-9, 2012

The initial phase of the storm started with a sudden commencement on October 8 (DOY=282) at 0700 UT when the Bz starts turning southward. After the initial

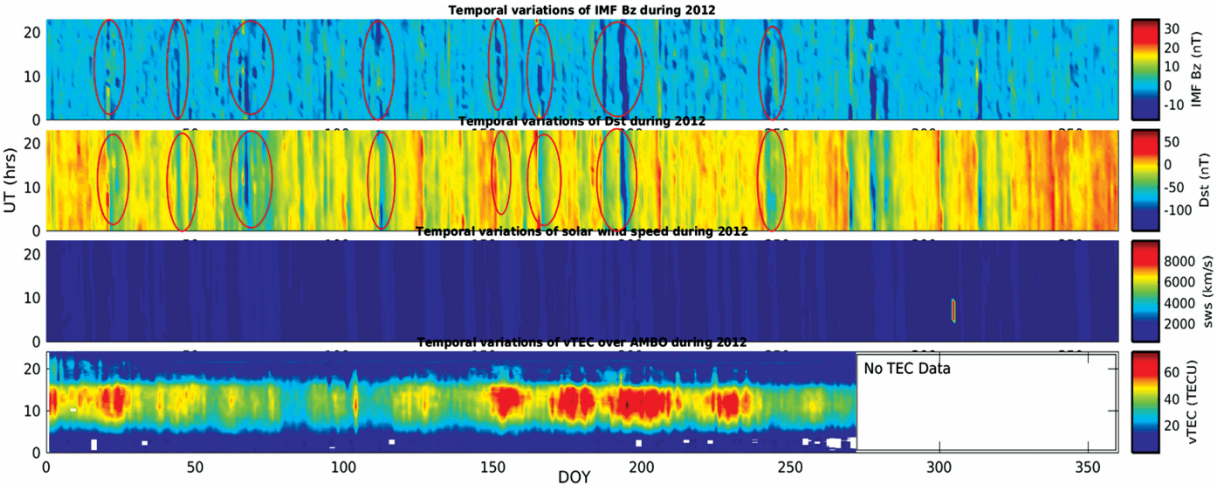

Fig. 9 — The variations of Bz, Dst, solar wind speed and the vTEC over Ambo in 2012. The circle in the figure shows the increment of IMF Bz and Dst index.

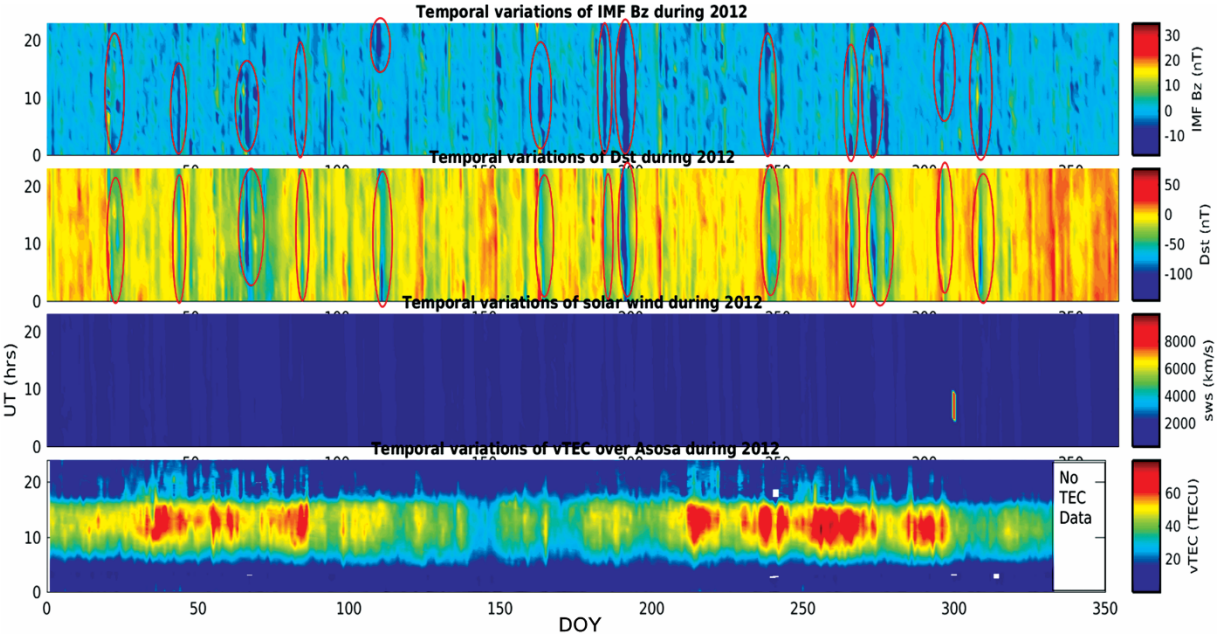

Fig. 10 — The variations of Bz, Dst, solar wind speed and the vTEC over Asosa in 2012. The circle in the figure shows the increment of IMF Bz and Dst index.

phase, Dst started becoming more negative during the main phase and reached -109 nT at 0800 UT on October 9, 2012. Bz starts turning southward at 0700 UT on October 8 and attains a maximum value of 15.6 nT at 0400 UT on October 9, 2012. The IMF Bz remained southward for almost 8 hours and then turned northward on October 10 at 0100 UT. For the analysis of October 8-9 storm during the initial phase and part of the main of this storm, the day time vTEC shows a positive response (about 55 TECU enhancement around 1000-1500 UT) followed by negative response in the post-sunset period a short enhancement of vTEC values at Bahir Dar, Arba Minch, Ambo, Asosa and Debark and in the night-time (at 2321 UT) shows negative response of vTEC was observed as shown in Figs 7, 8, 9, 10 and 11 respectively. In the afternoon and mid night period show a significant positive response (about 20 TECU). Post-midnight period as well as in morning periods show negative response.

3.3.5 Storm of November 14, 2012

On November 14 (DOY=319) the Dst value was -108 nT at 0700 UT, the Bz was -17.5 nT at 0600 UT and IMF Bz remained southward for 17 hours and then turned northward on October 15 at 0100 UT. For the analysis of the November 14, 2012 storm during the initial phase and part of the main phase at daytime vTEC shows a positive response (about 55 TECU enhancements around at 1000-1500 UT). In the post-sunset period, a short enhancement of vTEC values at Arba Minch and Debark observed. In the night-time (at 2321) shows negative response of vTEC observed as shown in Figs 8 and 11 at Arba Minch and Debark respectively. In the afternoon period and mid-night period, show a significant positive response (above 20 TECU). Post-midnight period as well as in morning periods show negative response at Arba Minch and Debark. However, during and after of this storm at Asosa shows negative storm as shown in Fig.10. Moreover, at Bahir Dar and Ambo have no vTEC data as shown in Figs 7 and 9.

3.4 Storm 2013

3.4.1 Strom of March 17, 2013

The initial phase of the storm started with a sudden commencement on March 17 (DOY=76) 2013 at 0500 UT when the Bz starts turning southward. After the initial phase, Dst started becoming more negative during the main phase and reach -132 nT at 0900 UT on March 17, 2013. The Bz starts southward at 0900 UT and attains a maximum value of -14 nT on March 17, 2013. IMF Bz remained southward for almost 17 hours and then turned northward at the end of day. In the main phase this storm, the day time vTEC shows a positive response (about 55 TECU) and in the post-sunset period a short enhancement of

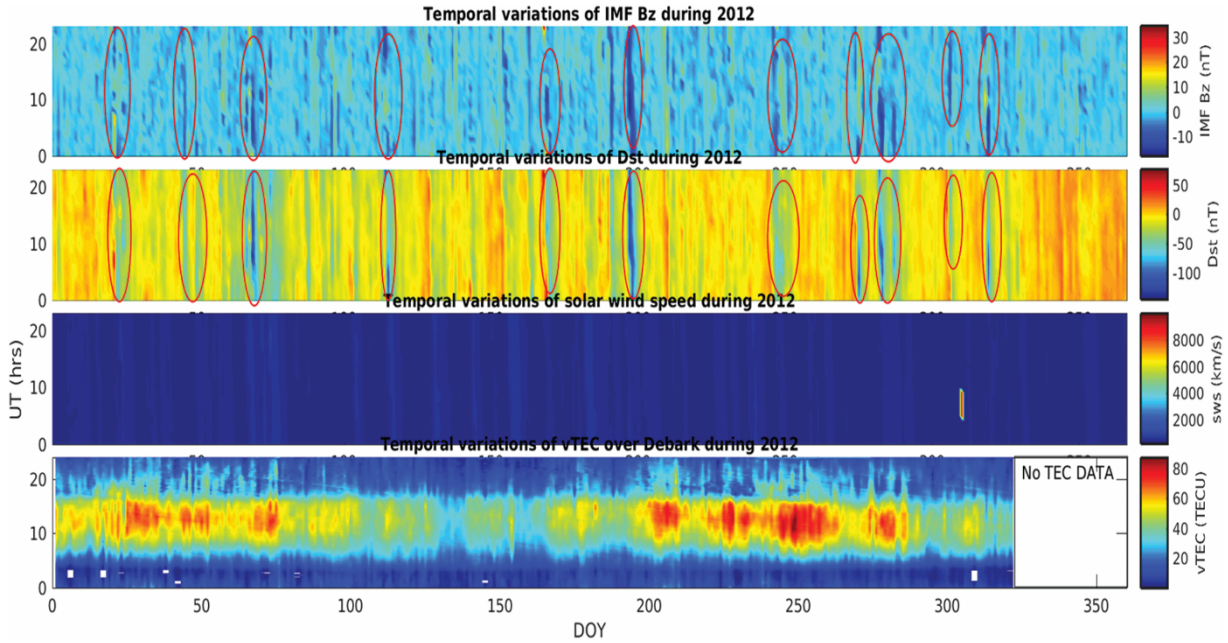

Fig. 11 — The variations of Bz, Dst, solar wind speed and the vTEC over Debark in 2012. The circle in the figure shows the increment of IMF Bz and Dst index.

vTEC (negative response) at Debark, Robe, Ambo and Asosa as shown Figs 12, 13, 14 and 15 respectively.

3.4.2 Storm of June 1 and 28, 2013

The initial phase of the storm started with a sudden commencement on June 1 (DOY=152) at 0100 UT when the Bz started turning southward. After the initial phase, Dst started becoming more negative during the main phase and reached -103 nT at 0400 UT on June 2, 2013. The Bz starts turned southward at 0900 UT and attains a maximum value of -16.7 nT at 0100 UT June 1, 2013. The IMF Bz remained southward for almost 26 hours and then turned northward on June 2 at 0500 UT. Then the storm on June 28 observed due to an interplanetary shock headed toward Earth is detected by solar wind around at 0200 UT on June 28, 2013. This shock caused by a solar halo coronal mass ejection observed by SOHO at 0200 UT on June 28, 2013.

The solar wind speed was so strong (1037km/s) and a sudden commencement on June 28 (DOY=179)

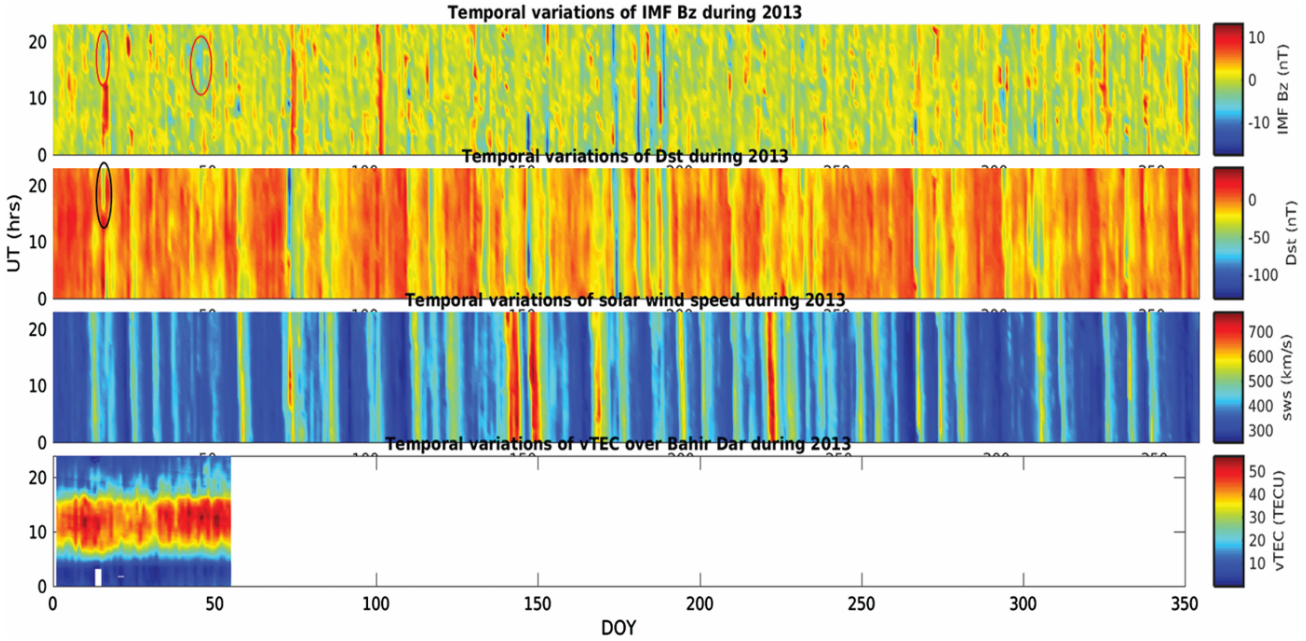

Fig. 12 — The variations of the Bz, Dst, solar wind speed and vTEC over Debark in 2013. The circle in the figure shows the increment of IMF Bz and Dst index.

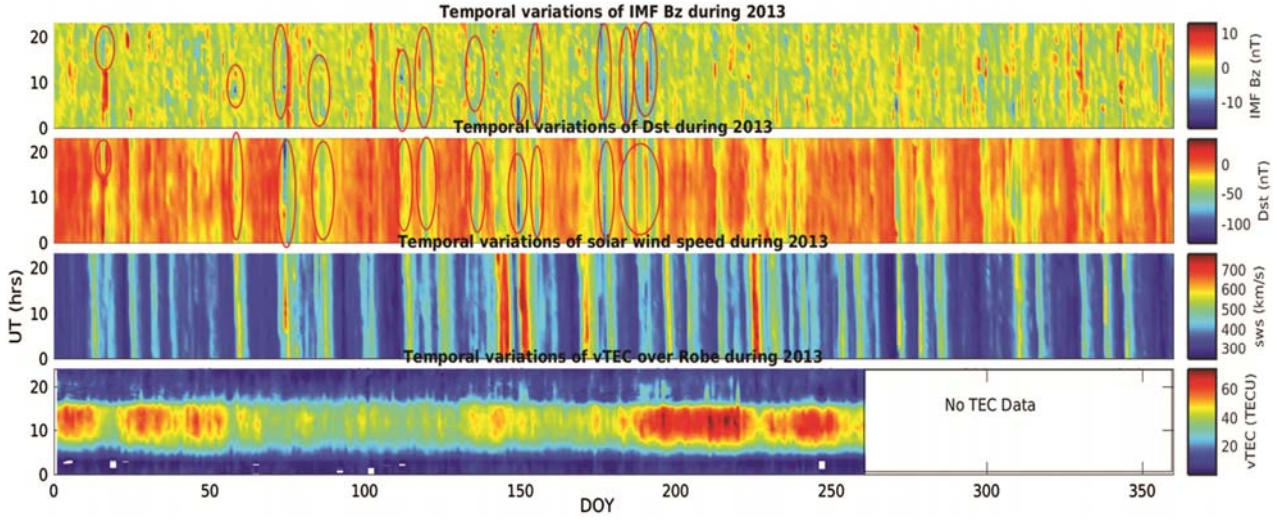

Fig. 13 — The variations of the Bz, Dst, solar wind speed and vTEC over Robe in 2013. The circle in the figure shows the increment of IMF Bz and Dst index.

at 0600 UT when the Bz started turning southward. The Dst value during the main phase is -102 nT at 0600 UT on June 29, 2013. Bz starts turning southward at 0900 UT and attained a maximum value of -12.0 nT at 2300 UT on June 28, 2013. IMF Bz remained southward for about 27 hours and then turned northward on June 30 at 0100 UT. The storm of June 1 and 28, 2013 during the initial phase and main phase the day time vTEC show a positive response (about 55 TECU) around 10.00-15.00 UT and followed by negative response in post-sunset period a short enhancement values at Debark (Fig. 12), Robe (Fig. 13), Ambo (Fig. 14), Asosa (Fig. 15) and Bahir Dar (Fig. 16) was observed. In the night time (at 2321 UT) shows negative response of vTEC; in the afternoon period and mid-night period show a significant negative response (about 20 TECU) in Bahir Dar, Robe, Ambo, Asosa and Debark as shown in the Figs 12, 13, 14, 15 and 16 respectively.

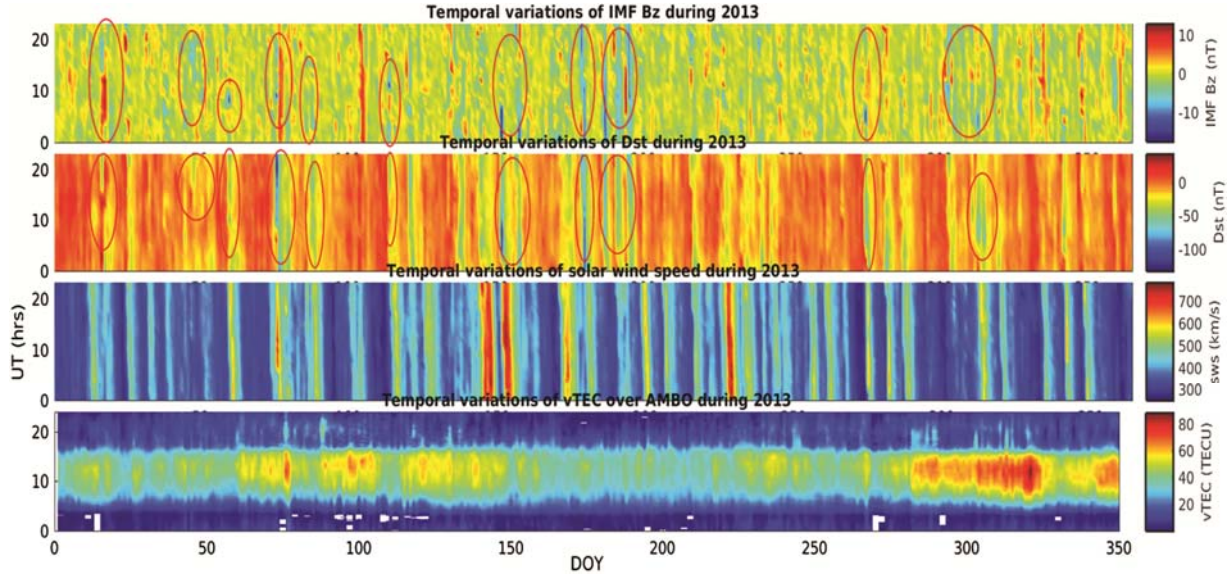

Fig. 14 — The variations of Bz, Dst, solar wind speed and the vTEC over Ambo in 2013. The circle in the figure shows the increment of IMF Bz and Dst index.

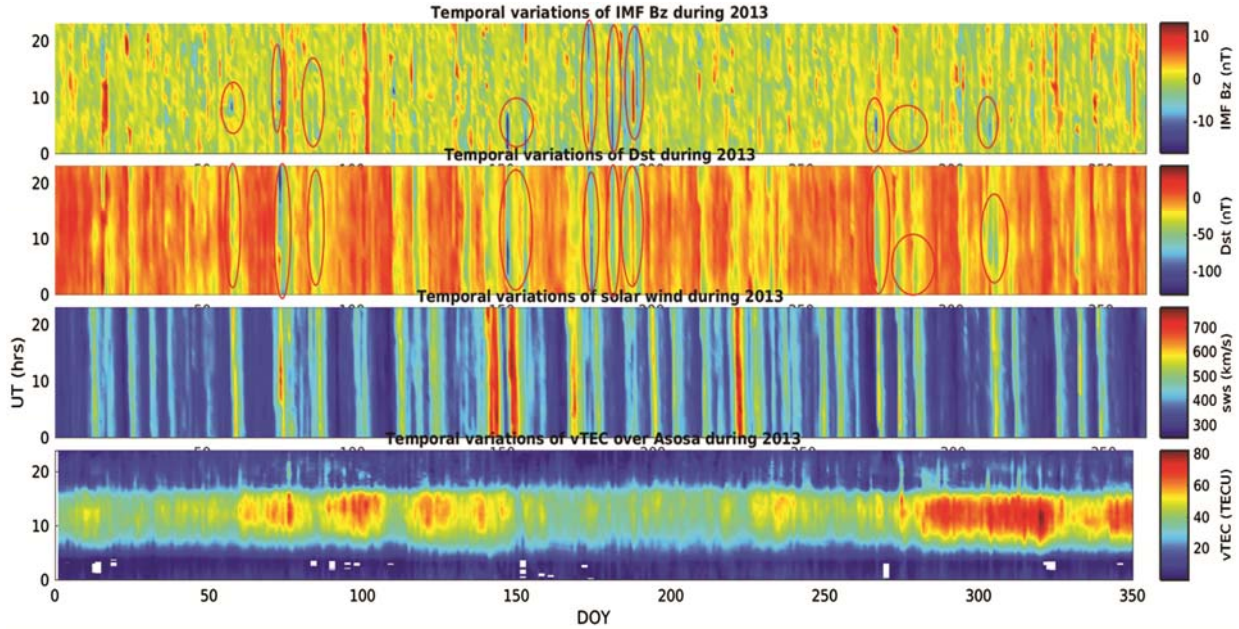

Fig. 15 — The variations of the Bz, Dst, solar wind speed and vTEC over Asosa in 2013. The circle in the figure shows the increment of IMF Bz and Dst index.

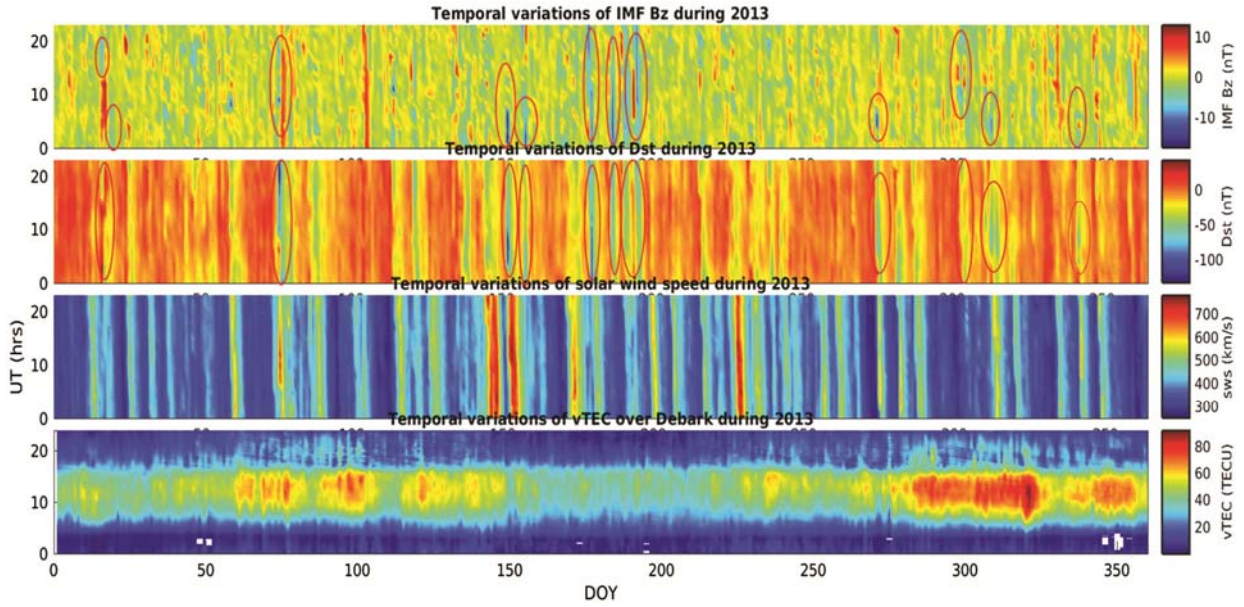

Fig. 16 — The variations of the Bz, Dst, solar wind speed and vTEC over Bahir Dar in 2013. The circle in the figure shows the increment of IMF Bz and Dst index.

4 Conclusions

The observational facts are consistent with the assumption of an equator ward propagation of the atmospheric ionospheric perturbation, which guided by thermospheric winds causing an effective uplifting of plasma on the dayside positive phase and a subsequent enhanced plasma loss due to the transport of composition changes negative phase. These results suggested that the different mechanisms might dominate the association between geomagnetic storms and ionospheric storms. In particular, the rapid strengthening of equatorial plasma up welling by enhanced eastward prompt penetrating electric field could be responsible for the positive storms associated with sudden geomagnetic storms, while the thermospheric heating leading to neutral composition changes and depletion in the ionospheric electron density could dominate negative ionospheric storms that are associated with gradual storm.

Daily averages of the Total Electron Content (TEC) of observations at Ethiopian GPS stations compared with Dts, a proxy for the geomagnetic activity at three times (0700-0800 UT, 1200-1300 UT and 1600-1700 UT). Comparisons made for data that include the full range of geomagnetic activity for data limited to quiet and moderate conditions. Most of the storms occurred due to the CMEs and turning of southward component of IMF, which is positive for all stations and the analysis concentrates on the recovery period during a positive response, is expected. When all the data are included, the correlations increase from morning to afternoon and comparisons of data with periods of days show significant correlations between TEC and Dst. 17 geomagnetic storms was occurred due to CMFs and IMF penetration and the most selected geomagnetic storm effect on the variation of the total electron content shows a positive response.

Acknowledgements

We would like to acknowledge and thank World Data Centre for Geomagnetism, Kyoto University, National Geophysical Data Centre (NGDC), Solar and Heliospheric Observatory (SOHO), National Oceanic and Atmospheric Administration (NOAA), Polar Operational Environmental Satellites (POES) for providing of solar activity and data sources.

References

1 Tsurutani BT, J. Geophys Res 113 (2008) A05311.
2 Cid C, Palacios J, Saiz E, Guerrero A & Cerrato Y, J. Space Weather Space Clim, 4 (2014) A28.
3 Chien H, Jann L, Tasi F & Chio C, Earth Planets Space, 59 (2000) 401.
4 Kelley M, Vlasov N, Foster C & Coster A, Geophys Res Lett, 31 (2004) L19809.
5 Fejer BG, Jensen J W, Kikuchi T, Abdu M A & Chau J L, J Geophys Res, 112 (2007) A10304.
6 Ngwira C N, Pulkkinen A, Wilder F D & Crowley G, Space Weather, 11 (2013) 121. Pulkkinen A, Bernaubeu E, Eichner J, Beggan C & Thomson A W P, Space Weather, 10 (2012) S04003.

7 Wei L S, Homeier N & Gannon, J Space Weather, 11 (2013) 451.
8 Loewe C A & Prolss G W, J Geophys Res, 102 (A7) (1997) 14209.
9 Gopalswamy N, Yashiro S & Akiyama S, J Geophys Res, 112 (2007) A06112.
10 Woodroffe J R, Morley S K, Jordanova V K, Henderson M G, Cowee M M & Gjerloev J G, Space Weather, 14 (2016).
11 Huang C, Foster J & Kelley M C, J Geophys Res, 110 (2005) A11309.
12 Mannucci A J, Tsurutani B T, Iijima B A, Komjathy A, Saito A, Gonzalez W D, Guarnieri F L, Kozyra J U & Skoug R, Geophys Res Lett, 32 (2005) L12S02.
13 Maruyama N, Richmond A D, Fuller-Rowell T J, Codrescu M V, Sazykin S, Toffoletto F R, Spiro R W & Millward G H, Geophys Res Lett, 32 (2007) L17105.
14 Endeshaw L, Astrophys Space Sci, 365 (2020) 49.
15 Gonzalez W D, Joselyn J A, Kamide Y, Kroehl H W, Tsurutani B T, Vasyliunas V M & Rostoker G, J Geophys Res, 99 (1994) 5771.
16 Zhao B, Wan W & Liu L, Ann Geophys, 23 (2005) 693.
17 Manju G, Kumar Pant T, Ravindran S & Sridharan R, Ann Geophys, 27 (2009) 2539.
18 Rama Rao P V S, Gopi Krishna S, Vara Prasad J, Prasad S N V S, Prasad D S V V D & Niranjan K, Ann Geophys, 27 (2009) 2101.
19 Astafyeva E, Ann Geophys, 27 (2009) 1175.
20 Vijaya Lekshmi D, Balan N, Tulasi Ram S & Liu J, J Geophys Res, 116 (2011) A11328.